

Effect of Electrodeposition Time on Microstructure, Morphology, and Optical Properties of CIGS Films

Erma Surya Yuliana¹, M. Abid Wahyudi², Robi Kurniawan³, Nasikhudin⁴, Nandang Mufti^{5*}

^{1,2,3,4,5}Department of Physics, Faculty of Mathematics and Natural Sciences, Universitas Negeri Malang, Jl. Semarang 5, Malang, 65145, Indonesia

⁵Center of Advanced Materials for Renewable Energy, Universitas Negeri Malang, Jl. Semarang No. 5, Malang, 65145, Indonesia

¹ermasy0407@gmail.com, ²wahyuabid99@gmail.com, ³robi.kurniawan.fmipa@um.ac.id, ⁴nasikhudin.fmipa@um.ac.id,

^{5*}nandang.mufti.fmipa@um.ac.id

ARTICLE INFO

Article history:

Received 19 September 2024

Revised 21 December 2024

Accepted 28 December 2024

Available online 30 January 2025



This is an open access article under the [CC BY-NC 4.0](https://creativecommons.org/licenses/by-nc/4.0/) license. Copyright © 2025 by Author. Published by Physical Society Indonesia

ABSTRACT

Solar cells based on crystalline structured materials such as CIGS (Copper Indium Gallium Selenide) have great potential to replace limited fossil energy sources. Optimization of CIGS solar cells was carried out using the electrodeposition method. Electrodeposition is carried out by dipping ITO and platinum substrate electrodes into a CIGS solution with a voltage of -2V for 5-15 minutes. Samples were characterized using XRD, SEM, and UV-Vis. Based on the XRD characterization results, the length of electrodeposition time increases the intensity in the hkl 211 and 112 planes, which indicates better CIGS crystallinity. The results of SEM characterization revealed that the CIGS particle size on the substrate surface can be deposited evenly, with the particle size getting smaller, namely 0.76, 0.68, and 0.32 μm . The SEM analysis also obtained the porosity values, namely 59.28, 64.05, and 68.34. The length of time for CIGS electrodeposition does not significantly affect the absorbance of the film in the UV light range, namely 300 - 350 nm. However, the CIGS band gap becomes larger, namely 3.66, 3.71, and 3.73 eV.

Keywords: CIGS; electrodeposition; thin film; electrodepositions time

ABSTRAK

Sel surya berbasis material berstruktur kristal seperti CIGS (Copper Indium Gallium Selenide) berpotensi besar menggantikan sumber energi fosil yang sifatnya terbatas. Optimasi solar sel CIGS dilakukan dengan metode elektrodeposisi. Elektrodeposisi dilakukan dengan mencelupkan elektroda berupa substrat ITO dan platina ke dalam larutan CIGS yang diberi tegangan -2V selama 5-15 menit. Sampel dikarakterisasi dengan menggunakan XRD, SEM, dan UV-Vis. Berdasarkan hasil karakterisasi XRD, lama waktu elektrodeposisi meningkatkan intensitas pada bidang hkl 211 dan 112, yang mengindikasikan kristalinitas CIGS yang semakin baik. Hasil karakterisasi SEM, diperoleh informasi bahwa ukuran partikel CIGS pada permukaan substrat dapat terdepositasi secara merata, dengan ukuran partikel yang semakin mengecil, yaitu 0,76; 0,68; dan 0,32 μm . Dari analisis SEM, juga didapatkan nilai porositas yaitu 59,28; 64,05; dan 68,34. Lama waktu elektrodeposisi CIGS tidak banyak mempengaruhi absorbansi film yang berada pada rentang sinar UV yaitu 300 – 350 nm. Akan tetapi, menggeser band gap CIGS menjadi semakin besar yaitu 3,66; 3,71; dan 3,73 eV.

Kata kunci: CIGS; elektrodeposisi; lapisan tipis; waktu elektrodeposisi

1. INTRODUCTION

Energy needs in Indonesia are dominated by energy originating from fossils such as oil, natural gas, and coal (Rahman et al., 2021). Meanwhile, the availability of fossil energy is dwindling, making researchers try to find new and renewable energy sources. Various types of renewable energy are available in nature, such as sunlight, sea waves, and wind (Ostergaard et al., 2022). Solar energy has great potential to meet the energy consumption needs of humans. The sun has an unlimited amount of energy (Kumar et al., 2023) and is environmentally friendly. Solar energy can be converted into electrical energy with a solar cell device. Solar cells work by absorbing photon

energy in specific wavelengths of sunlight, which results in electron jumps in the energy band of the solar cell material.

There are three generations of solar cells (Chukwuemeka et al., 2024); the first is generation one, which is silicon-based, for example, monocrystalline (Ray et al., 2023) and polycrystalline. These silicon-based solar cells are expensive. Apart from that, there are limitations to the use of this first-generation solar cell because of its thick dimensions. In the second generation, solar cells are based on thin films such as perovskite (Suo et al., 2025), amorphous silicon (Mufti et al., 2024), and CIGS (Mufti et al., 2020). This second-generation solar cell has high efficiency and can be deposited on a flexible substrate, making it easier to use. Meanwhile, the third generation is organic-based, such as Dye-sensitized solar cells (DSSC) (Yuliana et al., 2024). These solar cells are indeed very environmentally friendly, but their development is still limited to a lab scale and has not been widely produced on a mass scale (Nadhira et al., 2024). Various types of solar cell technology have been developed by researchers to date. One of them is the Copper Indium Gallium Diselenide (CIGS) solar cell (Adhikari et al., 2024). CIGS has attracted much interest from researchers because its performance can compete with first-generation solar cells sold commercially. The band gap value resulting from the Tauc graph plot has a value that is greater than the CIGS nanoparticles produced in previous research, namely 2.35 eV ~ 2.6 eV (Mankoshi et al., 2018). CIGS are usually produced using vacuum methods such as CVD (Kafashan et al., 2024), co-evaporation, and sputtering (Chamidah et al., 2024). However, this method requires expensive costs and high investment in equipment.

Until now, many non-vacuum methods have been used, such as spray coating (Park et al., 2025), spin coating (Dewi et al., 2020), knife coating, and electrodeposition (El-Bassri et al., 2025). The electrodeposition method is in great demand because it is easy to do with simple and cheap equipment but can produce a homogeneous CIGS layer. CIGS, using an electrodeposition method with SeO_2 as a selenium source, was done by a previous study (Rahmawati et al., 2022). Various electrodeposition parameters are determining factors in the properties of the resulting CIGS film. Several factors can influence the electrodeposition process, such as solvent, voltage during deposition (Saeed et al., 2021), pH of the CIGS solution (Oliveri et al., 2021), and distance of the electrode to the ITO substrate (Lara-Lara et al., 2019). However, not many studies have reported the effect of variations in deposition time on the resulting CIGS layer. Therefore, in this research, a study was carried out on the effect of electrodeposition time on the film structure, CIGS crystallinity, and absorbance of the CIGS film.

2. METHOD

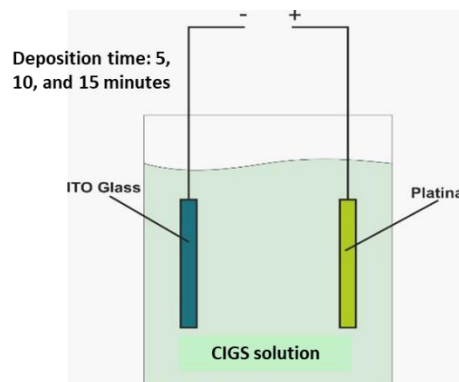


Figure 1. Illustration of CIGS deposition

First, 5 gr of selenium powder is dissolved in 2.5 mL of distilled water and then stirred at 150 rpm for 120 minutes at room temperature. After that, add 7.74 mL of hydrogen peroxide (H_2O_2) and stir at 150 rpm for 120 minutes. After the solution is formed, let it sit for 24 hours at room temperature. Filter the solution using filter paper. The filtered powder was dried using a hotplate for 60 minutes at 100°C . Second, the deposition of CIGS on the ITO substrate using the electrodeposition method. The precursors were 3 mM $\text{CuCl}_2 + 2\text{H}_2\text{O}$, 3 mM InCl_3 , 0.9 mM $\text{Ga}(\text{acac})_2$, and 8 mM SeO_2 (from the first step), which was dissolved in DI water, then HCl was added to adjust the pH of the solution to 1.7 and 2.2. In the electrodeposition process (Figure 1), time variations of 5 minutes (sample 1), 10 minutes (sample 2), and 15 minutes (sample 3) were given with a voltage of 2 volts. The resulting thin film was then annealed at 350°C for 30 minutes. The crystal area will produce peaks resulting from X-ray diffraction (XRD) from the XRD-E'xpert PRO instrument. The light used is a $\text{CuK}\alpha$ wavelength (λ) of 1.54060 Å with a step size of 0.02 degrees, and the graphic results are limited to a diffraction angle of 2θ scanned in the range 10 - 90° . The surface morphology of the CIGS was analyzed using scanning electron microscopy (SEM). The obtained SEM images were processed using ImageJ software to determine the particle size. The CIGS film's absorbance was obtained from the UV-Vis Analytical Jena Specord 200.

3. RESULT AND DISCUSSION

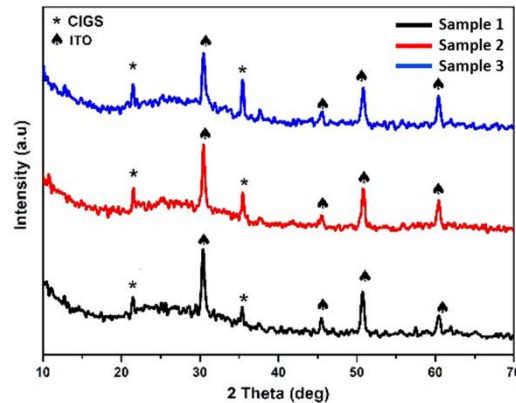


Figure 2. XRD pattern of CIGS film

Figure 2 shows the results of XRD characterization. Based on the analysis, the diffraction peak is dominated by ITO glass. The diffraction peaks at Bragg angles (2θ) of 30.35, 45.57, 50.80, and 60.45 correspond to (222), (431), (440), and (622) planes of the ITO lattice (Thirumoorthi et al., 2016), while 35.49 and 21.45 correspond to (211) and (112) CIGS lattice planes (Yang et al., 2016). The intensity of the CIGS peaks in these planes shows an increase. This increase in CIGS intensity indicates that crystallinity also increases (Wu et al., 2018). The hkl 112 and 211 fields are often identified as parameters of some phases, such as Cu-Se, CIS, CIGS, and so on (Farooq et al., 2019). Several studies reported that increasing the electrodeposition time could increase the Ga content in the CIGS formed (Mandati et al., 2019). The electrodeposition process basically involves flowing a negative voltage through the electrode so that the material which is a positive ion will move closer to the negative electrode, in this case the ITO substrate. The electrodeposition process, which is carried out in a short time, will not provide enough energy for the elements Cu, In, Ga and Se to bond perfectly and grow into crystals. This is what causes only two CIGS peaks to be detected in the XRD characterization results.

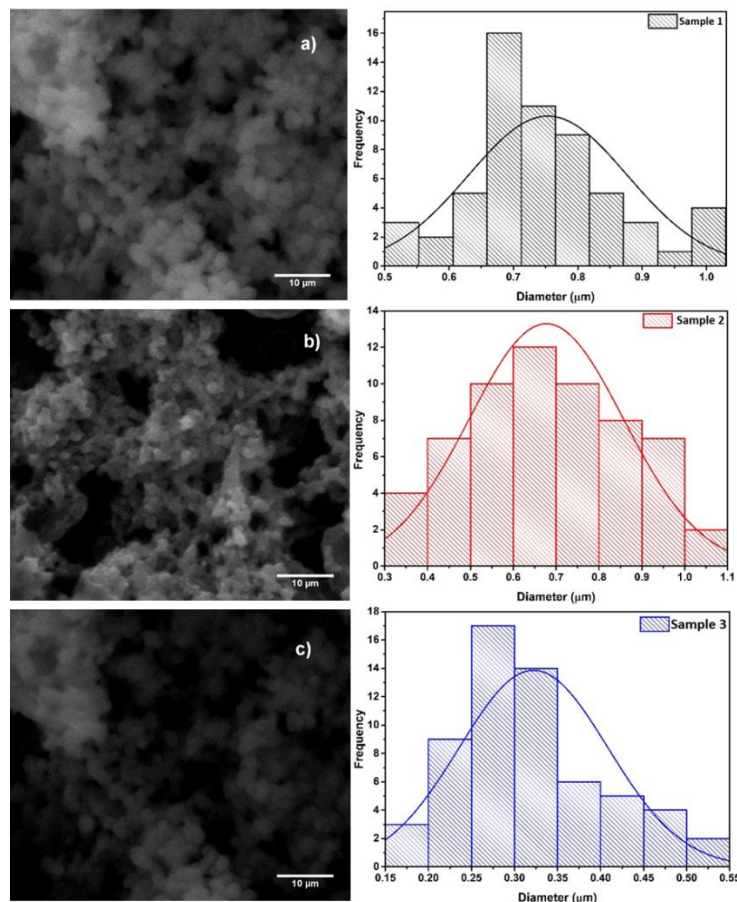


Figure 3. SEM images and particle size distribution of CIGS films (a) Sample 1, (b) sample 2, and (c) sample 3

Table 1. The porosity and particle size distribution of each CIGS film

Sample	Porosity (%)	Particle size distribution (nm)
Sample 1	59.28	0.76
Sample 2	64.05	0.68
Sample 3	68.34	0.32

Figures 3 (a)-(c) are the results of SEM testing magnified 100,000 times of CIGS thin films with varying deposition times of 5, 10, and 15 minutes. The morphology shown from each film is circular CIGS particles that agglomerate with different sizes. The average diameter of electrodeposited CIGS particles deposited for 5, 10, and 15 minutes, namely 0.76, 0.68, and 0.32 μm , respectively. Based on the results of this characterization, it can be seen that the longer the electrodeposition time, the smaller the CIGS particles that stick to the substrate with the same voltage. From the same SEM image, the porosity value of each sample can also be characterized. Porosity in the CIGS film layer is a substrate layer that is not coated with CIGS material of the area of the substrate coated with CIGS is thinner than the surrounding area (Mufti et al., 2022). The porosity and particle size distribution of each CIGS films are shown in Table 1. Based on the results of this analysis, the porosity value of CIGS films tends to increase. This increase in porosity is caused by increased CIGS nucleation along with the length of electrodeposition time used. When electrodeposition is carried out, the CIGS particles will stick to the surface of the conductive substrate. This attached particle arrangement will form pores on the substrate surface due to particle agglomeration. The longer the electrodeposition time, the agglomeration decreases due to the increase in grain boundaries. As a result, the particle size will become smaller, as shown in Figure 3. This smaller particle size distribution causes more pores to form. Electrodeposition carried out for 5 minutes resulted in a porosity of 59.28%. This result is lower compared to electrodeposition for 10 and 15 minutes, namely 64.05 and 68.34%. This increase in porosity due to nucleation was also reported (Lin et al., 2012). The porosity characterization of this bag shows that the longer the electrodeposition time, the more CIGS particle grain boundaries will increase, which causes a reduction in particle agglomeration, as reported in the SEM characterization results.

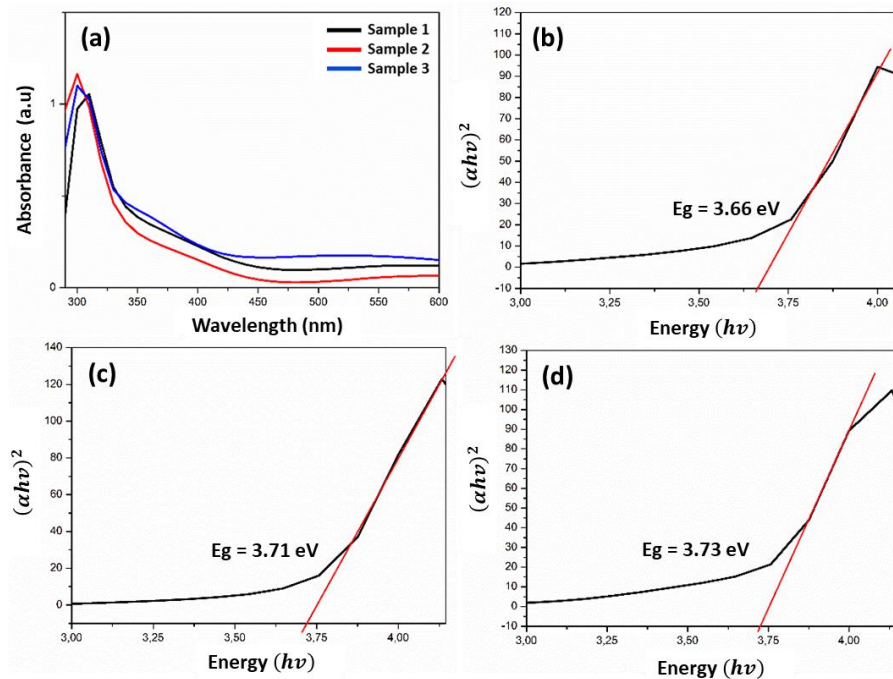


Figure 4. (a) UV-Vis spectra of CIGS films, and Tauc plot of (b) sample 1, (c) sample 2, (d) sample 3

Figure 4 (a) shows that CIGS film absorbs light maximally at a wavelength of 300 – 350 nm, which is the UV wavelength (Li et al., 2019). Adding a window layer and buffer layer with a wider band gap can increase the absorption of this wavelength range (Ghavami et al., 2020; Tobbeche et al., 2019). The amount of light spectrum that can be absorbed by a solar cell is determined by the band gap of the semiconductor. The type of band gap is highly dependent on the absorption coefficient. The absorption coefficient (α) can be calculated using the equation 1:

$$\alpha(\nu) = 2.303 \frac{A}{d} \quad (1)$$

and the relationship between photon energy and the absorption coefficient is formulated by equation 2:

$$\alpha h\nu = B(h\nu - E_g)^n \quad (2)$$

Meanwhile, photon energy ($h\nu$) is formulated using the following equation 3:

$$h\nu = h \frac{c}{\lambda} \quad (3)$$

where (ν) is the absorption coefficient (eV/m^2), A is the surface area, and d is the layer thickness (nm), $h\nu$ is the photon energy, B is the constant, E_g is the gap energy, and n is the exponent value which shows the nature of the band gap transition directly with a value of $1/2$, h is Planck's constant (6.626×10^{-34} Js), c is the speed of light in air (3×10^8 m/s), and λ is the wavelength (nm).

Based on the band gap data presented in Figure 4 (b) – (d), namely 3.66, 3.71, and 3.73 eV for films that were electrodeposited for 5, 10 and 15 minutes, respectively. The CIGS band gap value tends to increase with the length of CIGS film electrodeposition time. This is related to the longer the deposition time, the less Cu content is bound to the film layer. As Cu decreases, to reach chemical equilibrium, the Ga content will increase. This increase in Ga simultaneously increases the Ga/(In + Ga) ratio which specifically increases the CIGS band gap.

4. CONCLUSION

The CIGS film has been successfully coated using the electrodeposition method with a voltage of -2 V. In this research, varying electrodeposition times of 5, 10, and 15 minutes were carried out to determine the effect on the CIGS film's microstructure, morphology, and optical properties. The CIGS diffraction peaks were detected in the hkl 211 and 112 planes. Crystallinity increased over time with deposition time. The results of SEM analysis show that the particle sizes are 0.76, 0.68, and 0.32 μm , respectively. Meanwhile, UV-vis characterization shows that the absorbance and CIGS band gap are 3.66, 3.71, and 3.73 eV, respectively. The resulting CIGS film absorbs wavelengths best in the UV range.

5. ACKNOWLEDGEMENT

Universitas Negeri Malang supported this research through grant PNPB 2023 contract no. 5.4.568/UN32.20.1/LT/2023.

REFERENCES

- Adhikari, A., Acosta-Najarro, D. R., Fragoso-Medina, A. J., Reyes-Vallejo, O., Cano, F. J., Olvera Amador, M. D. L. L., & Subramaniam, V. (2024). Review on the developments in copper indium gallium diselenide (CIGSe)-based thin film photovoltaic devices. *Journal of Materials Science: Materials in Electronics*, 35(15), 1016. <https://doi.org/10.1007/s10854-024-12658-6>
- Chamidah, N. L. F., Mufti, N., Dewi, A. S., Permanasari, A. A., & Sunaryono, S. (2024). Effect of Temperature to Fabrication Cigs Solar Cell Using the Sputtering Method. In *E3S Web of Conferences* (Vol. 473, p. 01004). EDP Sciences. <https://doi.org/10.1051/e3sconf/202447301004>
- Chukwuemeka, E. J., Osita, N. A., Odira, A. O., & Chinwe, U. (2024). Performance and Stability evaluation of low-cost inorganic methyl ammonium lead iodide ($\text{CH}_3\text{NH}_3\text{PbI}_3$) Perovskite Solar cells enhanced with natural dyes from Cashew and Mango leaves. *Adv. J. Chem. Sect. A*, 7(1), 27-40.
- Dewi, A. S., Mufti, N., Arramel, A., Arrosyid, B. H., Sunaryono, S., & Aripriharta, A. (2020, April). Synthesis and characterization of CIGS/ZnO film by spin coating method for solar cell application. In *AIP Conference Proceedings* (Vol. 2231, No. 1). AIP Publishing. <https://doi.org/10.1063/5.0002493>
- El-Bassri, M., Almaggoussi, A., Abounadi, A., Boubakri, A., Koumya, Y., & Rajira, A. (2025). Effect of one-step electrodeposition time on the physical properties of tin sulfide thin films. *Applied Physics A*, 131(2), 124. <https://doi.org/10.1007/s00339-024-08220-0>
- Farooq, L., Alraeesi, A., & Al Zahmi, S. (2019). A review on the electrodeposition of CIGS thin-film solar cells. *IEOM Society International*, 26(28), 158-185.
- Ghavami, F., & Salehi, A. (2020). High-efficiency CIGS solar cell by optimization of doping concentration, thickness and energy band gap. *Modern Physics Letters B*, 34(04), 2050053. <https://doi.org/10.1142/S0217984920500530>.
- Kafashan, H., & Bahrami, A. (2024). CIGS solar cells using ZrS_2 as buffer layer: Numerical simulation. *Optik*, 298, 171594. <https://doi.org/10.1016/j.ijleo.2023.171594>
- Kumar, C. M. S., Singh, S., Gupta, M. K., Nimdeo, Y. M., Raushan, R., Deorankar, A. V., ... & Nannaware, A. D. (2023). Solar energy: A promising renewable source for meeting energy demand in Indian agriculture applications. *Sustainable Energy Technologies and Assessments*, 55, 102905. <https://doi.org/10.1016/j.seta.2022.102905>

- Lara-Lara, B., & Fernández, A. M. (2019). Growth improved of CIGS thin films by applying mechanical perturbations to the working electrode during the electrodeposition process. *Superlattices and Microstructures*, 128, 144-150. <https://doi.org/10.1016/j.spmi.2019.01.024>
- Li, Y., Lin, H., Zeng, J., Chen, J., & Chen, H. (2019). Enhance short-wavelength response of CIGS solar cell by CdSe quantum disks as luminescent down-shifting material. *Solar Energy*, 193, 303-308. <https://doi.org/10.1016/j.solener.2019.09.071>.
- Lin, Y. C., Lin, Z. Q., Shen, C. H., Wang, L. Q., Ha, C. T., & Peng, C. (2012). Cu (In, Ga) Se 2 films prepared by sputtering with a chalcopyrite Cu (In, Ga) Se 2 quaternary alloy and In targets. *Journal of Materials Science: Materials in Electronics*, 23, 493-500. <https://doi.org/10.1007/s10854-011-0424-8>.
- Mandati, S., Dey, S. R., Joshi, S. V., & Sarada, B. V. (2019). Two-dimensional CuIn1-xGaxSe2 nano-flakes by pulse electrodeposition for photovoltaic applications. *Solar Energy*, 181, 396-404. <https://doi.org/10.1016/j.solener.2019.02.022>.
- Mankoshi, M. A. K., Mustafa, F. I., & Hintaw, N. J. (2018, May). Effects of Annealing Temperature on Structural and Optical Properties of CIGS Thin Films for Using in Solar Cell Applications. In *Journal of Physics: Conference Series* (Vol. 1032, No. 1, p. 012019). IOP Publishing.
- Mufti, N., Amrillah, T., Taufiq, A., Diantoro, M., & Nur, H. (2020). Review of CIGS-based solar cells manufacturing by structural engineering. *Solar energy*, 207, 1146-1157. <https://doi.org/10.1016/j.solener.2020.07.065>
- Mufti, N., Ardilla, O. D., Yuliana, E. S., Wulandari, R. F., Taufiq, A., Setiyanto, H., ... & Septina, W. (2024). Improved performance of a SWCNT/ZnO nanostructure-integrated silicon thin-film solar cell: role of annealing temperature. *Materials Advances*, 5(22), 9018-9031. <https://doi.org/10.1039/D4MA00726C>
- Mufti, N., Dewi, A. S. P., Putri, R. K., Taufiq, A., & Nur, H. (2022). Selenization process in simple spray-coated CIGS film. *Ceramics International*, 48(15), 21194-21200. <https://doi.org/10.1016/j.ceramint.2022.04.015>.
- Nadhira, A. C. A., Mufti, N., Aziz, M. S., Sari, E. T., Yuliana, E. S., Abadi, M. T. H., ... & Setiyanto, H. (2024). The brief study of ZnO/PEDOT: PSS counter electrode in DSSC Based on solid electrolyte YSZ. *Materials Science for Energy Technologies*, 7, 309-317. <https://doi.org/10.1016/j.mset.2024.04.003>
- Oliveri, R. L., Patella, B., Di Pisa, F., Mangione, A., Aiello, G., & Inguanta, R. (2021). Fabrication of czts/cigs nanowire arrays by one-step electrodeposition for solar-cell application. *Materials*, 14(11), 2778. <https://doi.org/10.3390/ma14112778>
- Østergaard, P. A., Duic, N., Noorollahi, Y., & Kalogirou, S. (2022). Renewable energy for sustainable development. *Renewable energy*, 199, 1145-1152. <https://doi.org/10.1016/j.renene.2022.09.065>
- Park, H. K., & Jo, W. (2025). Flexible Cu (In, Ga) Se 2 photovoltaics for bending applications: advances from materials to panels. *Journal of Materials Chemistry C*. <https://doi.org/10.1039/D4TC04422C>
- Rahman, A., Dargusch, P., & Wadley, D. (2021). The political economy of oil supply in Indonesia and the implications for renewable energy development. *Renewable and Sustainable Energy Reviews*, 144, 111027. <https://doi.org/10.1016/j.rser.2021.111027>
- Rahmawati, H., Abadi, M. T. H., Zulaikah, S., & Mufti, N. (2022). Electrodeposition technique to fabrication CIGS using pure selenium and SeO2 as selenium source. *Malaysian Journal of Fundamental and Applied Sciences*, 18(3), 367-373. <https://doi.org/10.11113/mjfas.v18n3.2489>
- Ray, M., Kabir, M. F., Raihan, M., Noushad Bhuiyan, A. B. M., Akand, T., & Mohammad, N. (2023). Performance evaluation of monocrystalline and polycrystalline-based solar cell. *International Journal of Energy and Environmental Engineering*, 14(4), 949-960. <https://doi.org/10.1007/s40095-023-00558-0>
- Saeed, M., & González Peña, O. I. (2021). Mass transfer study on improved chemistry for electrodeposition of copper indium gallium selenide (Cigs) compound for photovoltaics applications. *Nanomaterials*, 11(5), 1222. <https://doi.org/10.3390/nano11051222>
- Suo, J., Yang, B., Bogachuk, D., Boschloo, G., & Hagfeldt, A. (2025). The dual use of SAM molecules for efficient and stable perovskite solar cells. *Advanced Energy Materials*, 15(2), 2400205. <https://doi.org/10.1002/aenm.202400205>
- Thirumoorthi, M., & Prakash, J. T. J. (2016). Structure, optical and electrical properties of indium tin oxide ultra thin films prepared by jet nebulizer spray pyrolysis technique. *Journal of Asian Ceramic Societies*, 4(1), 124-132. <https://doi.org/10.1016/j.jascer.2016.01.001>.
- Tobbeche, S., Kalache, S., Elbar, M., Kateb, M. N., & Serdouk, M. R. (2019). Improvement of the CIGS solar cell performance: structure based on a ZnS buffer layer. *Optical and Quantum Electronics*, 51, 1-13. <https://doi.org/10.1007/s11082-019-2000-z>.
- Wu, C. H., Wu, P. W., Chen, J. H., Kao, J. Y., & Hsu, C. Y. (2018). Effect of selenization processes on CIGS solar cell performance. *Journal of Nanoscience and Nanotechnology*, 18(7), 5074-5081. <https://doi.org/10.1166/jnn.2018.15279>.

- Yang, J., Du, H. W., Li, Y., Gao, M., Wan, Y. Z., Xu, F., & Ma, Z. Q. (2016). Structural defects and recombination behavior of excited carriers in Cu (In, Ga) Se₂ solar cells. *AIP Advances*, 6(8). <https://doi.org/10.1063/1.4961701>.
- Yuliana, E. S., Nadhira, A. C. A., Mufti, N., Diantoro, M., & Puspitasari, P. (2024). A Brief Study of the Carbon Counter Electrode for Photosensor based on DSSC. In *E3S Web of Conferences* (Vol. 473, p. 01005). EDP Sciences. <https://doi.org/10.1051/e3sconf/202447301005>